Melt processable cellulose fibres engineered for replacing oil-based thermoplastics

Chemical Engineering Journal 458 (2023) 141372

Contents lists available at ScienceDirect

Chemical Engineering Journal

journal homepage: www.elsevier.com/locate/cej

Melt processable cellulose fibres engineered for replacing oil-based thermoplastics

Giada Lo Re [a,d,*], Emile R. Engel [b], Linnea Björn [c,d], Manuel Guizar Sicairos [e], Marianne Liebi [d,e,f], Jan Wahlberg [g], Katarina Jonasson [a,g], Per A. Larsson [b,h,*]

[a] Industrial and Materials Science IMS, Chalmers University of Technology, SE-412 96 Gothenburg, Sweden
[b] Fibre and Polymer Technology, KTH Royal Institute of Technology, SE-100 44 Stockholm, Sweden
[c] Department of Physics, Chalmers University of Technology, Gothenburg SE-412 96, Sweden
[d] FibRe – Centre for Lignocellulose-Based Thermoplastics, Department of Physics, Chalmers University of Technology, SE-412 96 Gothenburg, Sweden
[e] Swiss Light Source, Paul Scherrer Institute, Villigen PSI, 5232, Switzerland
[f] Empa, Swiss Federal Laboratories for Materials Science and Technology, Centre for X-ray Analytics, St. Gallen 9014, Switzerland
[g] Tetra Pak, SE-221 86 Lund, Sweden
[h] FibRe – Centre for Lignocellulose-Based Thermoplastics, Department of Fibre and Polymer Technology, KTH Royal Institute of Technology, SE-100 44 Stockholm, Sweden

ARTICLE INFO

Keywords:
Dialcohol cellulose
Melt processing
Cellulose composite
Ethylene acrylic acid copolymer

ABSTRACT

If cellulosic materials are to replace materials derived from non-renewable resources, it is necessary to overcome intrinsic limitations such as fragility, permeability to gases, susceptibility to water vapour and poor three-dimensional shaping. Novel properties or the enhancement of existing properties are required to expand the applications of cellulosic materials and will create new market opportunities. Here we have overcome the well-known restrictions that impede melt-processing of high cellulose content composites. Cellulose fibres, partially derivatised to dialcohol cellulose, have been used to manufacture three-dimensional high-density materials by conventional melt processing techniques, with or without the addition of a thermoplastic polymer. This work demonstrates the use of melt processable chemically modified cellulose fibres in the preparation of a new generation of highly sustainable materials with tuneable properties that can be tailored for specific applications requiring complex three-dimensional parts.

1. Introduction

The cumulative global production of plastics is estimated to exceed 9 billion tonnes and based on current trends, 12 billion tonnes are expected to have accumulated in landfills or the natural environment by 2050 [1]. The development of new sustainable and biodegradable materials, as replacement candidates for non-biodegradable polymers, is a promising strategy to address this challenge.

Polymers melt processing is a widely used cost-effective procedure enabling large-scale production of geometrically complex objects (plastics). In a sustainable production horizon, melt processing emerges as a commercially viable product manufacturing technique, which, for example, does not require organic solvents, resulting in a health- and environment-friendly process.

Cellulose is a renewable resource and the most abundant biopolymer on Earth and has been identified as a key material in the sustainable society of tomorrow. Alongside biodegradability, cellulose exhibits several advantageous properties, including excellent stiffness, good barrier properties if low-enough porosity can be achieved and good processability as a two-dimensional material, such as paper or board [2].

Melt processing of cellulose-based materials, towards three-dimensional shaping, however, remains a challenge, despite the rapid expansion of research on this topic. Dry native cellulose fibres have limited ductility and cannot easily be formed into complex three-dimensional structures without creasing and folding. Furthermore, native cellulose fibres are characterised by a high glass transition temperature and typically degrade below their melting temperature; although extreme conditions such as high pressure in combination with energy in the form of high-intensity laser light have been demonstrated to be able to fuse cellulose fibres together [3]. Their thermal and

* Corresponding authors at: Industrial and Materials Science IMS, Chalmers University of Technology, SE-412 96 Gothenburg, Sweden.
E-mail addresses: giadal@chalmers.se (G. Lo Re), perl5@kth.se (P.A. Larsson).

https://doi.org/10.1016/j.cej.2023.141372
Received 3 November 2022; Received in revised form 23 December 2022; Accepted 6 January 2023
Available online 7 January 2023

viscoelastic properties hinder their possibility to flow. Thus, melt extrusion of non-fibrous thermoplastic cellulose derivatives, such as cellulose acetate [4], has been possible only within a narrow range of processing conditions and with the help of a plasticiser [5,6]. Dilute water dispersions of dissolved or nano-fibrillated cellulose can be injected by a syringe into a coagulation bath to form threads or filaments of enhanced mechanical strength [7,8]. Although such a process has been referred to as "wet extrusion" [7], it is not to be confused with conventional wet extrusion, as is widely employed in the food industry, or water-assisted melt processing, as described in the present work. For conventional cellulose fibres, extrusion and injection moulding requires addition of a large fraction of a thermoplastic polymer to enable their melt processing [9,10]. The intrinsic hydrophilicity of cellulose leads to compatibility issues with the more common hydrophobic polymer matrixes [11]. Composites of cellulose and conventional thermoplastic polymers have, therefore, typically suffered from pull-out and debonding [12,13], which undermines their final performance, particularly with respect to mechanical properties [14].

Bengtsson *et al.* [10] prepared a cellulose-fibre-reinforced polypropylene composite of up to 60 wt% fibres, achieving the highest cellulose fibre content included in a thermoplastic matrix thus far. The composite was prepared by extrusion, where pellets of cellulose were compounded with polypropylene. The extruded material exhibited a flexural modulus of 3 GPa, which is a threefold gain over the neat matrix.

To prevent phase separation and thermal degradation in melt compounded polyolefin composites, water-assisted melt compounding has been successfully used by, for example, the automotive industry for the preparation of clay-reinforced nylon and polyolefin composites [15–17], which is similar to the use of humid feeding for hemp fibres [18], and for micro-fibrillated cellulose [19]. Recently, a validation of a one-step wet feeding method (with initial water content higher than 50 wt%) was demonstrated by Lo Re *et al.* [20,21] as an effective sustainable approach for the melt compounding of cellulose fibre/polycaprolactone (PCL) biocomposites. Improved dispersion of the fibres, the preservation of their length, and a more pronounced fibrillation upon compounding resulted in a significant improvement in mechanical performance of the biocomposites. This approach has also enabled the production of high-performance cellulose nanofibril/PCL biocomposites, avoiding organic solvents or solvent exchange steps prior to melt processing [22,23].

Partial derivatisation of cellulosic fibres, by conversion of cellulose to dialcohol cellulose, (hereafter referred to as "modified fibres" for brevity) not only imparts higher ductility, but also hygro- and thermoplastic behaviour [24,25]. So far this modification has been used to demonstrate papers with outstanding strain-at-break, which have been hydroformed into complex double-curved structures (from flat substrates) [26]. However, trials have shown that this modified cellulose can potentially be used in melt-processing such as extrusion and injection moulding, suggesting significant potential for a new generation of cellulosic three-dimensional products [27]. Furthermore, by using fibres in the form of paper as the starting material for melt processing, large-scale production and possibly also recycling is made available through the paper and board industry.

Herein, we report straightforward melt processing of modified cellulose fibres and ethylene acrylic acid copolymer resin (EAA), which was selected to provide excellent adhesion to polar substrates without the need for a compatibilizer [28]. The incorporation of water as plasticiser allowed for the unprecedented melt processing of modified cellulose fibres without addition of a thermoplastic polymer such as EAA, which represents a major milestone towards the manufacture of three-dimensional high-density materials from cellulose. An example of industrially relevant manufacture of three-dimensional parts is presented here as a proof of concept.

2. Material and methods

Once-dried, bleached softwood kraft fibres (K46) were supplied by SCA Forest Products AB (Östrand pulp mill, Timrå, Sweden) and were mechanically beaten in a Voith mill to an energy input of 160 Wh kg^{-1} (about 30 SR), which increases the swelling of the fibres and makes them more flexible. Small-particle material (so-called fines) was removed by filtration through a 200-mesh metal screen, using a Britt Dynamic Drainage Jar (Paper Research Materials, Seattle, USA). Ethylene acrylic acid copolymer (EAA) (DOW Primacor 3540; polyethylene + 10 % ethylene acrylic acid). Sodium (meta)periodate was purchased from Alfa Aesar (98 %). Sodium borohydride and hydroxylamine hydrochloride were purchased from Sigma-Aldrich. Other chemicals such as sodium hydroxide, isopropanol (≥99.8 % purity) and sodium phosphate monobasic were all of analytical grade.

2.1. Cellulose modification

Bleached kraft fibres were chemically modified by sequential oxidation and reduction with sodium periodate and sodium borohydride, partly converting cellulose to dialcohol cellulose, according to a partly modified version of an earlier described protocol, known to increase the strain-at-break of papers; with a greater increase the higher the degree of conversion to dialcohol cellulose [24,25]. Two different sets of modified fibres were used: one prepared at small laboratory (gram) scale and one at larger (kilogram) scale using a batch reactor. The former was performed at KTH and the latter was performed as contract work at RISE Processum (Örnsköldsvik, Sweden). In both cases, the amount of aldehydes introduced was determined (after the oxidation step) by stoichiometric reaction with hydroxylamine hydrochloride [29,30].

The small-scale modification was performed under gentle agitation at room temperature by adding 5.4 g of sodium periodate per gram of fibre in a 4 g/l suspension containing 6.3 % isopropanol. After oxidation for 16, 24 or 32 h, the reaction was stopped by thorough washing with deionised water. This resulted in fibres with aldehyde contents of 3.7, 5.3 and 6.2 mmol g^{-1} of fibre, which, assuming pure cellulose, corresponds to a degree of modification of 32, 46 and 55 % (hereafter denoted Fibre32, Fibre46 and Fibre55). All aldehydes introduced were then reduced to primary alcohols by re-suspending the fibres to 4 g/l followed by addition of 0.5 g sodium borohydride per gram of fibres. To limit the increase in pH due to the alkaline borohydride, monobasic sodium phosphate was also added to an amount corresponding to 0.01 M. After four hours the reaction was stopped by thorough washing of the fibres.

The larger scale modification was performed in a stirred reactor using a modified protocol to reduce the consumption of chemicals as well as shortening the reaction time. By increasing the temperature to 50 °C and increasing the fibre consistency to 45 g/l, it was possible not only to reduce the periodate dosage to 1.4 g/g fibre but also the reaction time. Reaction times of 85 min and 105 min an aldehyde content of 4.5 mmol/g and 5.3 mmol/g, respectively, which corresponded to degrees of modification of 38 and 46 % (hereafter denoted Fibre38L and Fibre46L). The reduction of aldehydes was performed by adding 0.2 g of borohydride per gram of fibre in a 20 g/l suspension. The fibres were thoroughly washed after each reaction step.

2.2. Melt processing

Fig. 1 shows an overview of the method used to prepare the modified cellulose fibre-based composites. Prior to extrusion, EAA was added to a suitable amount of fibres at 100 wt% (reference) to 0 wt% EAA as a fraction of total dry mass. The fibres used were Fibre38L and Fibre55, conditioned at RH > 90 % for ty-pically-three days, depending on the degree of modification, resulting in a moisture content of 20–30 % [31]. This provided the suitable consistency of the system to render milder the shear stress and allow the complete water evaporation during the

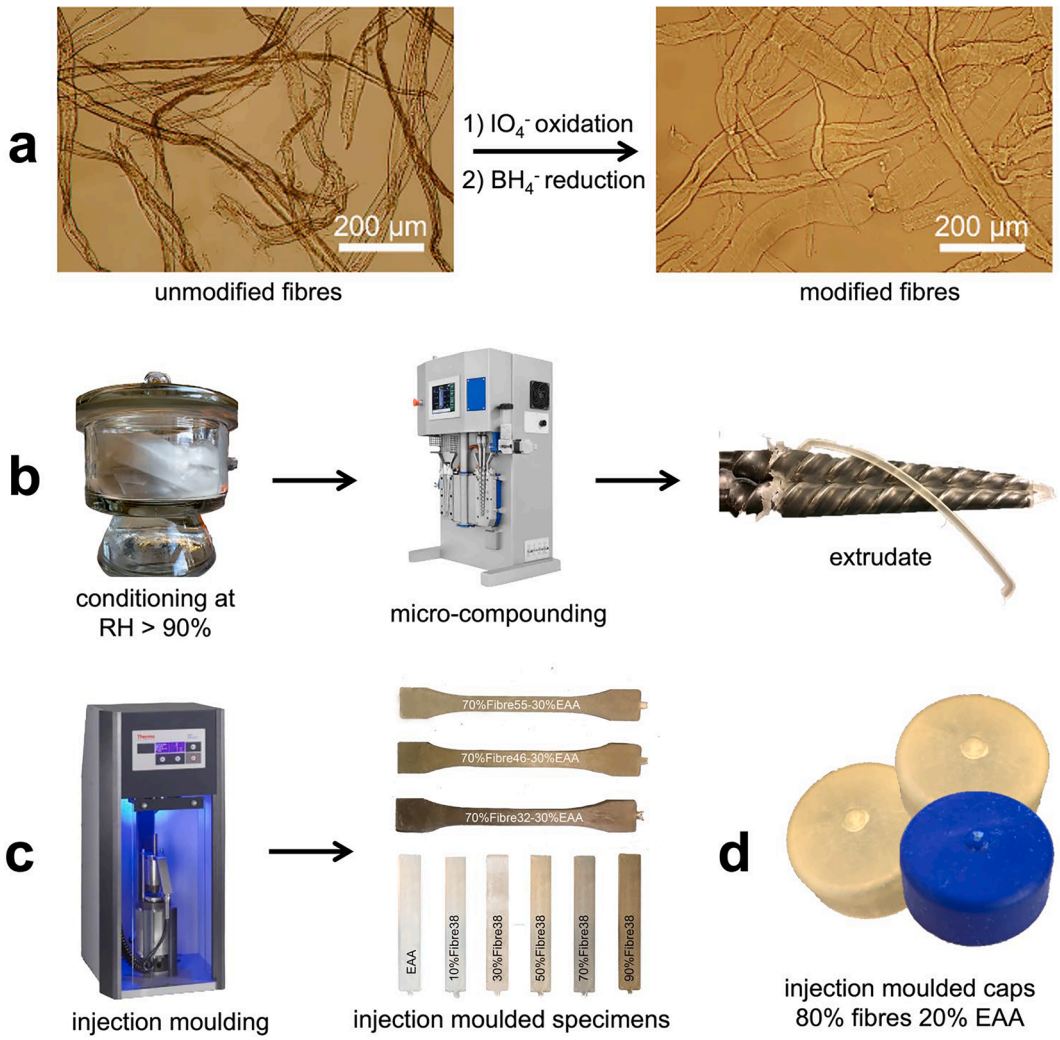

Fig. 1. Overview of the fibre modification and their melt processing: a) modification of cellulose fibres by partial derivatisation of cellulose to dialcohol cellulose by sequential periodate oxidation and borohydride reduction; b) dry- or moist-fed micro-compounding of composites (modified fibres and EAA) or modified fibres only to produce extruded filaments; c) injection moulding of test pieces for further mechanical characterisation; d) injection moulded bottle caps as an industrial proof of concept.

processing. The materials were melt processed at 80 °C or 120 °C using a Xplore Instruments Micro compounder MC 5, 5 ml corotating twin-screw micro-compounder (Heerlen, The Netherlands). The feeding was carried out at 30 rpm for 5 min and then at 60 rpm for 5 min, to make sure that the screw force, recorded during the processing, reached a constant value for all the materials. The axial force as screw force was recorded during the processing and it provides an indication of the viscosity of the system under the processing conditions. The achievement of a screw force plateau was interpreted as a steady-state condition without further substantial evaporation of water or fibre deterioration. After compounding, according to the standard ISO 527-2, dumbbell shaped (1BA) specimens and bars (60x10x1 mm^3) were prepared by injection moulding using a Thermo Scientific HAAKE MiniJet Pro (Thermo Fisher Scientific, Waltham, Massachusetts, USA) with the injection pressure of 1000 bar and an oven temperature of 140 °C and mould temperature of 40 °C. The composition of different samples, their initial and final water content, and acronym are displayed in Table 1.

As an industrial manufacturing proof of concept, bottle caps of a composite comprising 80 % modified fibres (Fibre46L) and 20 % EAA were injection moulded using a BOY 12A (Dr Boy GmbH & Co. KG, Neustadt, Germany). The injection moulding was done at a pressure of 2200–2400 bar, 130 °C and an injection speed of 14 $cm^3\ s^{-1}$. Coloured caps were also injection moulded using 2–3 wt% of Blue Masterbatch (supplied by Tetra Pak) pigment.

2.3. Morphological analysis

The morphology of the fibres and composites was analysed by scanning electron microscopy (SEM) and X-ray tomography.

High-resolution SEM micrographs were acquired by using a Hitachi SEM S-4800 (Tokyo, Japan) with an accelerating voltage of 1 kV. Tensile fractured surfaces of the neat inject-moulded dumbbell-shaped specimens of EAA and the composite were analysed after Pt/Pd (60/40) sputtering for 20 s at a current of 80 µA using a Cressington 208HR sputter coater (Watford, UK) prior to imaging. Mixtures of cellulose fibres in aqueous dispersion were deposited onto carbon-coated 400 mesh copper grids (TED PELLA, Redding, California, USA) and examined in the microscope after drying.

X-ray tomography data were collected on a Xradia MicroXCT-200 (Carl Zeiss X-ray Microscopy, Pleasanton, California, USA) with X-ray focal spot size 7 µm. Samples of the melt processed composites and fibre-only materials were cut from injection-moulded test pieces. Instrument settings for high resolution scans were as follows: source voltage of 80 kV, source current of 100 µA, source-sample distance of 25 mm, detector-sample distance of 10 mm, field of view approx.1 mm, pixel size of 0.4851 µm, exposure time of 20 s, and 1289 projections. For low

resolution scans, the settings were the same, except for a reduced field of view of 2 mm, a voxel size of 1.921 μm and exposure time 2 s.

2.4. Wide-angle synchrotron X-ray scattering

For assessing the homogeneity and fibre orientation in the injected samples, their structural characteristics in different volumes were investigated by scanning wide-angle X-ray scattering (WAXS). The samples were prepared by cutting 50 μm slices of the injection molded materials using a RMC MT-XL ultramicrotome equipped with a glass knife (Boeckeler Instruments, Tucson, Arizona, USA). The WAXS imaging experiments were performed at the cSAXS beamline X12SA of the Swiss Light Source, Paul Scherrer Institute, Switzerland. Measurements where preformed using an X-ray energy of 12.4 keV and a focused beam of 42x4 μm^2. A Pilatus 2 M detector was used to record the scattering images and was placed at 250 mm from the sample. The step size used during the scanning WAXS measurements was 5x40 μm^2, with the smaller step size in the thickness direction of the injection moulded samples. The exposure time for each measuring point was 60 ms.

Scattering patterns were analysed using the cSAXS MATLAB analysis package [32]. The scattering intensity and degree of orientation in each scattering pattern was calculated in specific q-ranges according to Bunk et al. [33]. For analysing the EAA, a q-region of 24.8–25.9 nm^{-1} corresponding to the (0 2 0)-peak, was used, and for analysing the modified cellulose, a q-region of 10.2–10.7 nm^{-1}, corresponding to the (1 1 0)-peak, was used. The q-regions were chosen to minimise the overlap between scattering signal from EAA and modified cellulose (Fig. S9).

2.5. Thermal analysis

Thermogravimetric analysis (TGA) and differential scanning calorimetry (DSC) were carried out using a Mettler Toledo TGA/DSC 1 (Stockholm, Sweden) under nitrogen atmosphere. For DSC the temperature was ramped from room temperature to 180 °C, then to −50 °C and again to 180 °C, at a heating rate of 10 °C min^{-1}. The glass transition inflection point temperature (T_g), melting peak temperature (T_m) and melting enthalpy (ΔH_m) were determined from the second heating (-50 to 180 °C). All TGA data were measured with a temperature ramp from 70 to 600 °C at 10 °C min^{-1} on samples dried overnight under vacuum at 40 °C.

2.6. Mechanical characterisation

Tensile tests of the fibres-based composites were performed on samples conditioned for at least three days at 23 °C and 50 % RH using a single column Instron 5944 (Norwood, Massachusetts, USA) tensile micro tester with a load force of 2 kN according to the ASTM D638-14 standard. Tensile testing was performed with a gauge length of 30 mm and a deformation rate of 15 mm min^{-1}. Five replicates were performed for each composition. The fibre-based composites were analysed by dynamic mechanical thermal analysis (DMTA) on samples conditioned for at least three days at 23 °C and 50 % RH using a TA Instruments DMA Q800 (New Castle, Delaware, USA), accordingly with the ASTM D5023-07 standard. The DMTA measurements were carried out in three-point bending mode, at a constant frequency (1 Hz), amplitude of 10 μm, and a temperature ramp from −20 to 70 °C at a heating rate of 2 °C min^{-1}. Three replicates were performed for each composite formulation.

2.7. Barrier properties

Oxygen transmission rate (OTR) measurements were performed at an oxygen level of 21 % using a MOCON OX-TRAN 2/21 (AMETEK MOCON, Berwyn, Pennsylvania, USA). The samples were injection moulded caps (80 % modified fibres and 20 % EAA) as described above. The top and side thickness of the caps were 0.80 mm and 0.87 mm, respectively. Caps were glued to a special holder, using epoxy, and measured at three different conditions: 23 °C and 50 % RH; 23 °C and 80 % RH; 38 °C and 90 % RH. Readings were taken when the OTR reached a plateau. Commercially available (supplied by Tetra Pak) caps of low-density polyethylene (LDPE) were used as reference. The oxygen permeability typically reported for LDPE is 220 cm^3 mm m^{-2} atm^{-1} day^{-1}, allowing for estimates of the permeability in the fibre-based caps.

3. Results and discussion

3.1. Chemical modification of fibres

An overview of the fibre modification process and after-following melt processing is presented in Fig. 1. Partial derivatisation of the cellulose in fibres to dialcohol cellulose was achieved by periodate oxidation followed by borohydride reduction (Fig. 1a). The optical micrographs suggest that partial derivatisation to dialcohol cellulose increases the swelling propensity of the fibres. This observation is consistent with evidence in literature of a slight increase in water retention value for similar fibres at 11 % degree of modification, *i.e.* a degree of modification much lower than that used in our work [34]. The increase in swelling propensity is explained by a reduction in crystallinity, and greater availability of hydroxy groups, which interact strongly with water [25,34]. The properties of the modified fibres have been shown to be consistent with a core–shell model where cellulose nanofibrils within the modified fibres comprise a crystalline core of unreacted cellulose surrounded by a disordered shell of dialcohol cellulose [24,35–37].

Under atmospheric conditions, unmodified cellulose fibres do not soften upon heating because thermal degradation occurs at temperatures well below their T_g. It has previously been demonstrated that partial modification to dialcohol cellulose reduces the T_g, such that heating under atmospheric conditions softens the fibres without significant degradation. Additionally, water acts as a plasticiser of the modified fibres; increasing moisture content further depresses their T_g [25,26,34].

3.2. Effect of fibre content on the melt processing

Considering thermal properties and the effect of moisture, the modified fibres were either dried before feeding into a micro-compounder or conditioned at > 90 % RH for wet feeding (Fig. 1b). The fibres were either manually mixed with EAA pellets before feeding or processed without such a polymer (100 % fibre). Water-assisted melt processing (from moisture by conditioning at > 90 % RH) [20,21] exploits the plasticising effect of moisture and reduces the number of steps before melt processing. To investigate the effect of fibre content on processability, composites of EAA containing varying amounts of modified fibre, from 10 %Fibre38L-90 %EAA to 90 %Fibre38L-10 % EAA, were melt processed. Once extrudates had been obtained from micro-compounding, samples were injection moulded into bars or dumbbell-shaped test pieces (Fig. 1c) for further mechanical characterisation. As a proof of concept for industrial applications, bottle caps were injection moulded from a composite containing 80 % Fibre46L and 20 % EAA (Fig. 1d).

The axial force measured during micro-compounding reflects the viscosity of the system, at the selected processing conditions. Axial force curves for neat EAA and the composites are reported in Fig. 2a. The axial force curve of EAA after initial increase during the feeding, reach the typical plateau of a thermostable thermoplastic polymer, indicating a constant viscosity for EAA during the entire processing time. The relatively low axial force required for the melt compounding of neat EAA, slightly higher than 1 kN, supports a good melt processability and relatively low viscosity of EAA at the processing conditions, because of its relatively low glass transition temperature, low melting temperature, and linear polyethylene-like structure [38]. An increased fibre content resulted in a greater viscosity, pointed out by the progressively

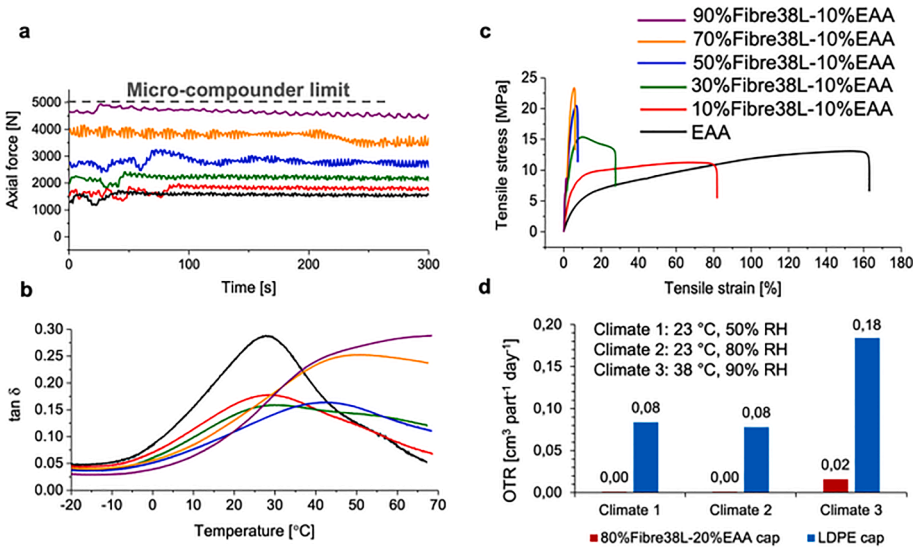

Fig. 2. Flow, mechanical and barrier properties for neat EAA and its composites with Fibre38L: a) axial force curves for micro-compounding of the neat polymer and fibre-based composites at 120 °C; b) stress–strain curves from tensile testing; c) tan δ as a function of temperature measured by DMTA; d) Results of OTR measurements on injection-moulded bottle caps.

increasing axial force, which also is an indication of a good interfacial interaction, fibres of the EAA with the modified fibres, *i.e.* good wetting of the fibres [38]. For 90 %Fibre38L-10 %EAA, the axial force approached the 5 kN, maximum force limit of the micro-compounder. Degradation would likely be associated with a variation in viscosity, which should be observed as a decrease in axial force. However, only at very high fibre contents (>70 wt%) a slight negative slope is observed in the axial force curves in Fig. 2, while the other composites (<70 wt% fibre) ~~a~~ are reaching a plateau, suggesting that no additional significant degradation occurred during processing.

Tensile testing was carried out on injection-moulded dumbbell-shaped test pieces of the materials after micro-compounding. The resultant stress–strain curves (Fig. 2b) and measured properties (Table S2) indicate that increasing fibre content improves strength but reduces ductility. With increasing fibre content there is an increase in Young's modulus from 0.38 ± 0.01 GPa for 10 %Fibre38L-90 %EAA to 3.21 ± 0.14 GPa for 70 %Fibre38L-30 %EAA and an increase in tensile strength. However, there is a substantial loss in elongation-at-break from 56 % for 10 %Fibre38L-90 %EAA to 5.3 % for 70 %Fibre38L-30 %EAA. Our work focuses on the tensile properties of melt processed (compounded and injection moulded) dialcohol cellulose fibres 3D shaped in Dumbbells' specimens. Therefore, a direct comparison with the properties of bidimensional papers based on not melt processed cellulose fibres or nanofibrils (CNF) would be inaccurate.

DMTA measurements in three-point bending mode were carried out on injection-moulded bars. The damping factor, tan δ,(Fig. 2b) and flexural storage and loss moduli (Fig. S1) are presented as a function of temperature and additional parameters, determined from the DMTA curves, are summarised in Table S3. The transition temperatures as the peak of loss moduli for the higher fibre content composites showed higher values, indicating a sensible reduction in the molecular mobility of EAA. At these fibre contents, we propose that an interpenetrating network of EAA, and possibly a secondary network of modified fibres, exists, which accounts for the significant change in viscoelastic behaviour of the composites. The shape of the damping curve showed a transitional behaviour for the 50 wt% fibre composites, with a peak shifted to higher temperature. The 70, 90 and 100 wt% fibre-based composites showed a damping curve monotonically increasing, typical of a continuous fibre network. This trend is consistent with a typical dynamic viscoelastic behaviour of cellulose. During the temperature sweep (Fig. S1), the higher the fibre content, the higher the storage moduli. Consistently, increasing the modified fibre content, the glass transition of the composites, determined as the peak of the loss moduli, shifted towards higher temperatures, indicating a more and more constrained molecular mobility. The latter result highlights the thermoplastic nature of the modified cellulose used in this work [39]. The neat EAA matrix displayed the typical behaviour of a semicrystalline polymer where the modulus remained approximately constant at temperatures below the T_g, followed by a gradual decrease to a plateau typical of the rubbery state above the T_g (Fig. S1). The addition of modified fibres reinforced the EAA matrix as indicated by the increase of the flexural storage modulus. A super-linear increase in modulus, as a function of fibre content, was evaluated at fibre contents higher than 30 wt% (Fig. S2). The values for the 50, 70 and 90 wt% of fibres were 3.9, 6.8 and 9.2 GPa, respectively, at −20 °C, and decreased gradually above room temperature, upon heating. These results are consistent with good adhesive properties of ionomers such as EAA towards the hydrophilic surfaces of the modified fibres [38,40].

TGA revealed an effect of the increased shear stress on the thermal stability of the materials. The first derivative of the TGA curve (the so-called "DTG curve") (Fig. S3), shows a first peak, related to the degradation of fibres (around 340 to 360 °C), that broadens with increasing cellulose content, while the second peak around 450 to 475 °C corresponds to degradation of the EAA matrix. For 50 %Fibre38L-50 %EAA a small shoulder in the DTG curve is noticeable at approximately 288 °C, which also can be attributed to the typical degradation pattern of the cellulose fibres. The onset temperature of the thermal degradation showed a mutual protective effect of the fibre-EAA composites compared with the pristine materials (summarised in Table S4). Up to 70 % fibre content, the damping factor increased, in line with the TGA results which indicates lower thermostability of cellulose fibres within the composites (increasing the fibre content leads to increase the axial force, *i.e.,* the viscosity, hence leading to higher shear forces which would result in higher fibre shortening). These results support the DMTA data and underline the good affinity between the fibres and thermoplastic matrix. For the two highest fibre contents, the slight decrease observed for both the degradation temperatures was conceivably ascribed to the increased shear stress during the compounding, consistent with the registered axial force values (Fig. 2a). The DSC data (Fig. S4, and Table S5) shows that the EAA enthalpy of melting in the composites decreases with the increasing fibre content. This decrease is non-linear, as a consequence of a strong EAA–modified cellulose

interaction, hindering the mobility of the EAA, *i.e.,* limiting its crystallization.

3.3. Effect of degree of modification on the melt processing

To investigate the effect of degree of modification, 70 %Fibre32-30 %EAA, 70 %Fibre46-30 %EAA and 70 %Fibre55-30 %EAA composites were micro-compounded and compared (Fig. 3g–l). The axial force values measured during micro-compounding are provided in Table S1. Evidently, the viscosity decreases with increasing degree of modification, which is consistent with previous observations that the ductility of sheets increases and T_g decreases with increasing degree of modification [25]. The results imply that, for melt processing of composites, an increasing degree of modification of the fibres reduces the required amount of added thermoplastic polymer, *i.e.* the higher the degree of modification the easier the processability. Based on this observation, we then investigated the possibility of processing modified fibres without any addition of EAA. The three samples investigated were dry-fed Fibre55, water-assisted Fibre38L and water-assisted Fibre55. Water was introduced by conditioning the samples at a relative humidity>90 %. Dry-fed 100 %Fibre55 was micro-compounded at 120 °C and even at low screw speed (30 RPM) the axial force approached the limit of the extruder. For wet-fed 100 %Fibre38L and 100 %Fibre55, the increased moisture content resulted in lower viscosities (*i.e.* lower axial force values) during processing, which reduced the friction from shearing. For 100 %Fibre55, this feeding allowed for successful melt processing at lower temperature (80 °C) and higher screw speed (60 RPM). A filament obtained from water-assisted melt processing of 100 %Fibre55 is shown in Fig. 1b and Fig. S5a. Soaking the processed material in water for 24 h caused it to re-swell, resulting in a material that resembled pulp (Fig. S5b). The fibre morphology is indeed affected by the melt compounding but is also to a large extent preserved during the melt processing (compounding and injection moulding), suggesting interesting prospects for recycling of these materials.

It was not possible to measure the mechanical properties for the material obtained from water-assisted melt processing of 100 % Fibre38L, because of the challenge in the extraction of the injected specimen from the mould. Mechanical properties obtained from tensile testing of the fibre-only materials, “100 %Fibre55 dry” and “100 % Fibre55 90 % RH”, are provided in Table S2. These materials showed high level of rigidity (Young’s moduli of 10.1 and 12.2 GPa, respectively) as compared with the composites (0.1–3.2 GPa), but also very brittle, with low elongation-at-break (<0.5 %). The reason for this brittleness is subject for further research. It can be suggested to be a result of a loss of the percolation of the plasticizer phase, both in the case of composites with EAA content lower than 30 % and when water is used as plasticizer. The equilibrium of water content during the conditioning of the specimens could also affect the mechanical performance. Both the formulated hypotheses are currently under evaluation.

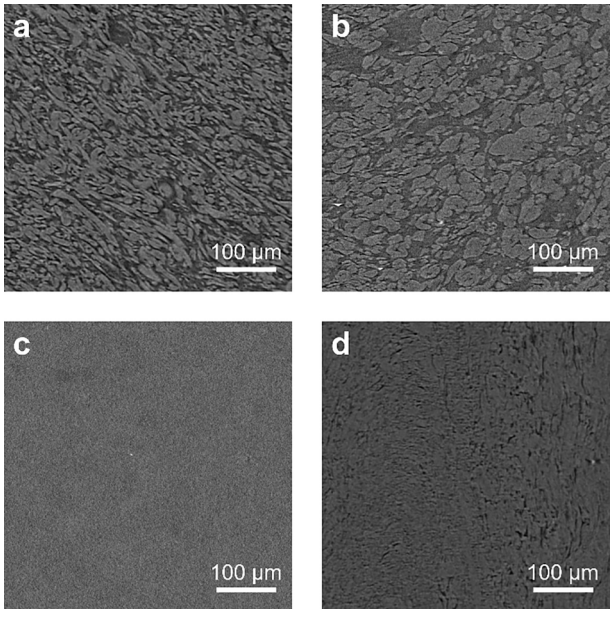

Fig. 3. X-ray tomography images of cross-sections of injection-moulded samples: a) 70 %Fibre32-30 %EAA; b) 70 %Fibre55-30 %EAA; c) Fibre55; d) 80 % Fibre46L-20 %EAA bottle cap.

3.4. Proof of concept: injection moulded caps for packaging

As a proof of concept towards the industrial manufacture of three-dimensional objects based on these materials, injection moulded bottle caps (Fig. 1d) were prepared with a composition of 80 % Fibre46L and 20 % EAA, using industrial scale injection moulding equipment. Measurements of oxygen permeability showed that these materials have excellent gas barrier properties (Fig. 2d), outperforming pure LDPE even at high relative humidity. Note that the typical oxygen permeability of LDPE is 220 cm^3 mm m^{-2} atm^{-1} day^{-1}, while our fibre composite even under high temperature and moisture has a permeability below 20 cm^3 mm m^{-2} atm^{-1} day^{-1}. For the potential scale-up of this demonstrator, it is worth noting that the periodate used in the modification of the cellulose fibres is too expensive to simply be considered a consumable and would need to be regenerated. This can be done both electrochemically [41], chemically by a stronger oxidant such as hypochlorite [42], or even by ozone [43], where the latter has been demonstrated to have very high recovery efficiency under the right conditions.

3.5. Structural characterisation at multiple length scales

SEM and X-ray tomography were used to investigate the morphological characteristics of the processed materials. SEM images of cryo-fractured surfaces (Fig. S6) indicate that the fibres are well dispersed within the EAA matrix. There is no evidence of fibre pull-out or fibre–matrix debonding. X-ray tomography of a fibres-only melt processed sample (100 %Fibre55 conditioned at > 90 % RH) (Fig. 3c) showed insufficient contrast to distinguish individual fibre particles. However, the X-ray tomography images of injection-moulded samples of 70 %Fibre32-30 %EAA and 70 %Fibre55-30 %EAA presented in Fig. 2a and Fig. 2b, respectively, suggests that the modified fibres remain at least partially intact as macroscopic particles at these compositions. Additionally, there are no indications of fibre clustering since the fibres appear to be homogeneously distributed throughout the EAA matrix. Excellent homogeneity is also evident in the image of the 80 %Fibre46L-20 %EAA sample (bottle cap), (Fig. 2d) although it is not readily possible to distinguish individual fibres from the matrix. Three-dimensional renderings from the X-ray tomography are provided in Fig. S7.

To further assess the structure of EAA and cellulose within the composites, as well as their degree of orientation, samples with different degree of modification and different composition were analysed by scanning WAXS. Fig. 4 shows the degree of orientation calculated in composites containing 10 wt%, 30 wt% and 50 wt% Fibre38L, and 70 % Fibre32, Fibre46 and Fibre55. The scattering intensity of the (020) diffraction peak of EAA and the (110) diffraction peak of cellulose (see Fig. S9) were used to analyse the distribution of cellulose fibres across the injection moulded samples. For all fibre compositions, the intensity shows a homogeneous profile across each sample cross-section, without any indication of a layered structure (Fig. S9). This indicates good dispersion and homogeneous distribution of the cellulose, and hence the fibres (and any fibre fragments), in the EAA matrix. The degree of orientation of the polymer in the plots (Fig. 3a–l) shows a layered structure with higher degree of orientation close to the edges (EAA peak). Both the higher orientation of the polymer in the close neighbourhood of the wall and the transverse orientation originates from the

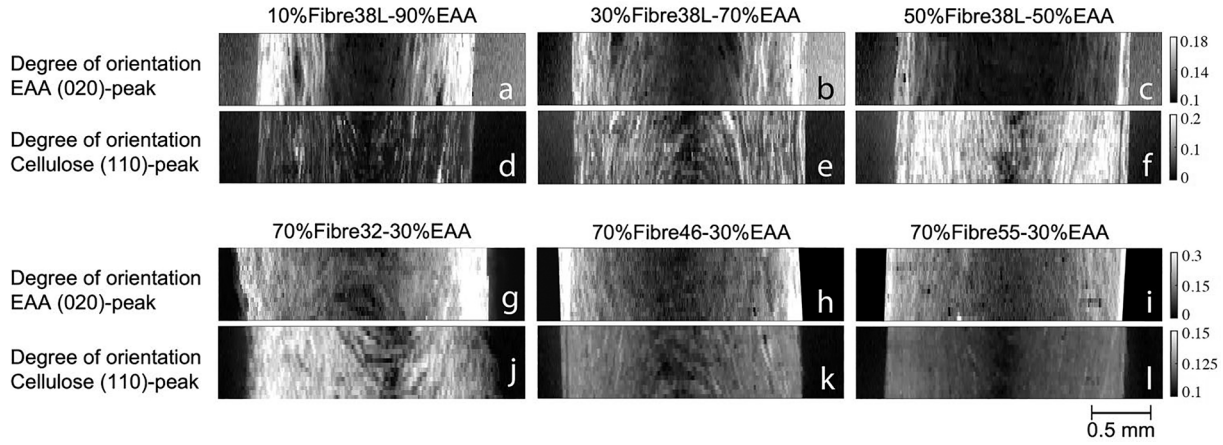

Fig. 4. Images of the degree of orientation calculated from scanning WAXS measurements of 10 %Fibre38L-90 %EAA, 30 %Fibre38L-70 %EAA and 50 %Fibre38L-50 %EAArelated to: a–c) the EAA (020)-peak, d–f) the Cellulose (110)-peak, and degree of orientation calculated from WAXS measurements of 70 %Fibre32-30 %EAA, 70 %Fibre46-30 %EAA and 70 %Fibre55-30 %EAA related to: g–i) the EAA (020)-peak, j–l) the cellulose (110)-peak.

fountain-type flow in the advancing front region during the injection moulding process [44,45]. The degree of orientation of the EAA (020)-peak (Fig. 3a–c) shows that the samples with a lower amount of cellulose have a higher degree of orientation compared to the samples with a higher amount of cellulose, consistently with a strong interaction between EAA and modified cellulose which hinder the EAA mobility. In particular, the oriented shear layer close to the edge of the injection moulded samples are broader when the cellulose fibre concentration is low. This indicates that the cellulose interferes with the propensity of the polymer to form ordered structures, causing the degree of orientation to decrease as the cellulose content increases. The calculations of the degree of orientation for the cellulose (110)-peak (Fig. 4d–f) show the opposite trend where the cellulose has a higher degree of orientation in samples with a high amount of cellulose. The results imply that cellulose (and consequently the fibres) can be more oriented at a high fibre fraction, which corresponds to a more viscous system with higher shear forces. This result is also in line with a strong interaction between EAA and modified cellulose which on one hand hinder the EAA orientation, and on the other hand, at low EAA concentration, it serves as a plasticiser, allowing the modified cellulose fibres to align more easily in the direction of the flow (under stronger shear forces). Fig. 3 shows that at a high fibre fraction there is a high degree of orientation of the cellulose through the sample, except from a thin less oriented core layer.

In addition, scanning WAXS was used to investigate how the degree of modification influences homogeneity and degree of orientation of unmodified cellulose in the injection moulded parts (Fig. S9). A homogenous distribution was found for all degree of modifications indicating good mixing. While the degree of orientation was unaffected for the EAA (020)-peak (Fig. S9 g–i), the degree of orientation obtained from the cellulose (110) peak indicated a loss of orientation with increasing degree of modification (Fig. S9 j–l). The reason behind this observation is a subject for further studies. However, it could be hypothesized that a lower shear force is needed to injection mould the part when the degree of modification increases.

4. Conclusions

It has been demonstrated here that melt processing of modified cellulose fibres (partially modified to dialcohol cellulose) is possible for fibres only and for composites of remarkably high fibre content. This finding points at a wider exploitation of cellulosic fibres in previously excluded applications, which require complex 3D shapes. In this study, we have provided a simple but effective demonstrator in terms of a screw cap suitable for a bottle or a liquid board packaging.

Micro-compounding was achieved at temperatures of 80–120 °C with an axial force of<5 kN. For dry-fed composites with EAA, viscosity during micro-compounding increased with increasing fibre content. However, analysis by SEM, X-ray tomography and WAXS indicated that the fibres were well distributed within the polymer matrix (no substantial aggregation) and fibre pull-out or debonding had not occurred. WAXS analysis further revealed that higher cellulose content was associated with a higher degree of orientation of cellulose fibres within the matrix.

Incorporation of moisture, by conditioning at high humidity, has a plasticising effect on the modified fibres. Melt processing *without* addition of a thermoplastic polymer was achieved for fibres at relative high degree of modification: 38 and 55 %. In these instances, it was essential to incorporate water as a plasticiser.

CRediT authorship contribution statement

Giada Lo Re: Conceptualization, Methodology, Validation, Formal analysis, Investigation, Data curation, Writing – review & editing, Supervision, Funding acquisition. **Emile R. Engel:** Data curation, Writing – review & editing. **Linnea Björn:** Wide-angle synchrotron X-ray scattering analysis. **Manuel Guizar Sicairos:** Wide-angle synchrotron X-ray scattering analysis. **Marianne Liebi:** Wide-angle synchrotron X-ray scattering analysis. **Jan Wahlberg:** Pilot-scale production and barrier properties. **Katarina Jonasson:** Pilot-scale production and barrier properties. **Per A. Larsson:** Conceptualization, Methodology, Writing – review & editing, Supervision, Funding acquisition.

Declaration of Competing Interest

The authors declare that they have no known competing financial interests or personal relationships that could have appeared to influence the work reported in this paper.

Data availability

Data will be made available on request.

Acknowledgments

Financial support for the original experimental work from the Swedish Innovation Agency VINNOVA, BioInnovation ProDAC (Reference number 2021-02094) is acknowledged.

This project was further supported by Treesearch: a platform for collaboration on new materials from the forest, in association with Tetra Pak, as well as FibRe: a competence centre for design for lignocellulose-

based thermoplastics research, partly funded by the Swedish Innovation Agency VINNOVA (grant number 2019-00047).

GLR and ML thank the Genie programme at Chalmers University of Technology for financial support.

The authors thank Fredrik Adås of RISE Research Institutes of Sweden for X-ray tomography analysis.

Appendix A. Supplementary data

Electronic Supplementary Information: Summary of axial force values measured during micro-compounding; Summary of mechanical properties determined from tensile testing; Summary of mechanical properties determined using DMTA; Flexural storage modulus and loss modulus as a function of temperature measured using DMTA; Young and flexural storage moduli at -20 °C and 25 °C as a function of the fibre volumetric fraction; TGA and relative DTG thermograms of extruded EAA and composites; Summary of TGA results; DSC second heating scans of extruded EAA and composites; Summary of DSC results; Water-assisted fibre-only micro-compounded samples of 100%Fibre55 immediately after micro-compounding and after soaking the micro-compounded material in water for 24 h; SEM micrographs of tensile fractured surfaces of neat EAA and composites; X-ray tomography three-dimensional renderings for injection moulded; WAXS results showing integrated intensity as a function of scattering vector q for EAA, fibre composites and modified cellulose; Results from scanning WAXS intensities of 10%Fibre38L-90%EAA, 30%Fibre38L-70%EAA and 50% Fibre38L-50%EAA, 70%Fibre32-30%EAA, 70%Fibre46-30%EAA and 70%Fibre55-30%EAA showing the symmetric intensity of the EAA (020)-peak, the symmetric intensity calculated for the cellulose (110)-peak. Supplementary data to this article can be found online at https://doi.org/10.1016/j.cej.2023.141372.

References

[1] R. Geyer, J.R. Jambeck, K.L. Law, Production, use, and fate of all plastics ever made, Sci. Adv. 3 (2017) 25–29.
[2] R.J. Moon, A. Martini, J. Nairn, J. Simonsen, J. Youngblood, Cellulose nanomaterials review: structure, properties and nanocomposites, Chem. Soc. Rev. 40 (2011) 3941–3994.
[3] J. Schroeter, F. Felix, Melting cellulose, Cellulose 12 (2) (2005) 159–165.
[4] R. Quintana, O. Persenaire, L. Bonnaud, P. Dubois, Recent advances in (reactive) melt processing of cellulose acetate and related biodegradable bio-compositions, Polym. Chem. 3 (2012) 591–595.
[5] X. Dreux, J.C. Majesté, C. Carrot, A. Argoud, C. Vergelati, Viscoelastic behaviour of cellulose acetate/triacetin blends by rheology in the melt state, Carbohydr. Polym. 222 (2019), 114973.
[6] A. Charvet, C. Vergelati, D.R. Long, Mechanical and ultimate properties of injection molded cellulose acetate/plasticizer materials, Carbohydr. Polym. 204 (2019) 182–189.
[7] A. Walther, J.V.I. Timonen, I. Díez, A. Laukkanen, O. Ikkala, Multifunctional high-performance biofibers based on wet-extrusion of renewable native cellulose nanofibrils, Adv. Mater. 23 (26) (2011) 2924–2928.
[8] K.M.O. Håkansson, A.B. Fall, F. Lundell, S. Yu, C. Krywka, S.V. Roth, G. Santoro, M. P. Kvick, L. Wittberg, L. Wågberg, L.D. Söderberg, Hydrodynamic alignment and assembly of nanofibrils resulting in strong cellulose filaments, Nat. Commun. 5 (2014) 4018.
[9] A.K. Bledzki, J. Gassan, Composites reinforced with cellulose based fibres, Prog. Polym. Sci. 24 (1999) 221–274.
[10] M. Bengtsson, M.L. Baillif, K. Oksman, Extrusion and mechanical properties of highly filled cellulose fibre–polypropylene composites, Compos. Part A Appl. Sci. Manuf. 38 (8) (2007) 1922–1931.
[11] M.N. Belgacem, A. Gandini, The surface modification of cellulose fibres for use as reinforcing elements in composite materials, Compos. Interfaces 12 (2005) 41–75.
[12] G. Lo Re, M. Morreale, R. Scaffaro, F.P. La Mantia, Kenaf-filled biodegradable composites: rheological and mechanical behaviour, Polym. Int. 61 (2012) 1542–1548.
[13] S. Spinella, G. Lo Re, B. Liu, J. Dorgan, Y. Habibi, P. Leclère, J.M. Raquez, P. Dubois, R.A. Gross, Polylactide/cellulose nanocrystal nanocomposites: Efficient routes for nanofiber modification and effects of nanofiber chemistry on PLA reinforcement, Polymer 65 (2015) 9–17.
[14] E. Petinakis, L. Yu, G. Edward, K. Dean, H. Liu, A.D. Scully, Effect of matrix–particle interfacial adhesion on the mechanical properties of poly (lactic acid)/wood-flour micro-composites, J. Polym. Environ. 17 (2009) 83–94.
[15] J. Karger-Kocsis, Á. Kmetty, L. Lendvai, S.X. Drakopoulos, T. Bárány, Water-assisted production of thermoplastic nanocomposites: a review, Materials 8 (2015) 72–95.
[16] D.D.J. Rousseaux, N. Sallem-Idrissi, A.C. Baudouin, J. Devaux, P. Godard, J. Marchand-Brynaert, M. Sclavons, Water-assisted production of thermoplastic nanocomposites, Polymer 52 (2011) 443–451.
[17] J. Soulestin, N. Quiévy, M. Sclavons, J. Devaux, Polyolefins–biofibre composites: A new way for an industrial production, Polym. Eng. Sci. 47 (2007) 467–476.
[18] J. Beaugrand, F. Berzin, Lignocellulosic fiber reinforced composites: Influence of compounding conditions on defibrization and mechanical properties, J. Appl. Polym. Sci. 128 (2013) 1227–1238.
[19] K. Suzuki, H. Okumura, K. Kitagawa, S. Sato, A.N. Nakagaito, H. Yano, Development of continuous process enabling nanofibrillation of pulp and melt compounding, Cellulose 20 (2013) 201–210.
[20] G. Lo Re, S. Spinella, A. Boujemaoui, F. Vilaseca, P.T. Larsson, F. Adås, L. A. Berglund, Poly(ε-caprolactone) Biocomposites Based on Acetylated Cellulose Fibers and Wet Compounding for Improved Mechanical Performance, ACS Sustain. Chem. Eng. 6 (2018) 6753–6760.
[21] G. Lo Re, V. Sessini, Wet feeding approach for cellulosic materials/PCL Biocomposites, ACS Symp. Ser. 1304 (2018) 209–226.
[22] G. Lo Re, J. Engström, Q. Wu, E. Malmström, U.W. Gedde, R.T. Olsson, L. Berglund, Improved Cellulose Nanofibril Dispersion in Melt-Processed Polycaprolactone Nanocomposites by a Latex-Mediated Interphase and Wet Feeding as LDPE Alternative, ACS Appl. Nano Mater. 1 (2018) 2669–2677.
[23] T. Kaldéus, A. Träger, L.A. Berglund, E. Malmström, G. Lo Re, Molecular Engineering of the Cellulose-Poly(Caprolactone) Bio-Nanocomposite Interface by Reactive Amphiphilic Copolymer Nanoparticles, ACS Nano 13 (6) (2019) 6409–6420.
[24] P.A. Larsson, L.A. Berglund, L. Wågberg, Cellulose 21 (2014) 323–333.
[25] P.A. Larsson, L. Wågberg, Towards natural-fibre-based thermoplastic films produced by conventional papermaking, Green Chem. 18 (11) (2016) 3324–3333.
[26] E. Linvill, P.A. Larsson, S. Östlund, Advanced three-dimensional paper structures: Mechanical characterization and forming of sheets made from modified cellulose fibers, Mater. Des. 128 (2017) 231–240.
[27] P. Larsson G. Lo Re Melt-Processed Material with High Cellulose Fibre Content WO 2018/135994 A1, 2018.
[28] I. Novák, S.J. Florián, Study of the change in polarity of polypropylene modified in bulk by polar copolymers, Mater. Sci. 36 (2001) 4863–4867.
[29] H. Zhao, N.D. Heindel, Determination of Degree of Substitution of Formyl Groups in Polyaldehyde Dextran by the Hydroxylamine Hydrochloride Method, Pharm. Res. 8 (1991) 400–402.
[30] P.A. Larsson, M. Gimåker, L. Wågberg, The influence of periodate oxidation on the moisture sorptivity and dimensional stability of paper, Cellulose 15 (6) (2008) 837–847.
[31] L. Salmén, P.A. Larsson, On the origin of sorption hysteresis in cellulosic materials, Carbohydr. Polym. 182 (2018) 15–20.
[32] Scanning SAXS Software Package, https://www.psi.ch/en/sls/csaxs/software.
[33] O. Bunk, M. Bech, T.H. Jensen, R. Feidenhans'l, T. Binderup, A. Menzel, F. Pfeiffer, Multimodal x-ray scatter imaging, New J. Phys. 11 (12) (2009) 123016.
[34] V. López Durán, P.A. Larsson, L. Wågberg, Chemical modification of cellulose-rich fibres to clarify the influence of the chemical structure on the physical and mechanical properties of cellulose fibres and thereof made sheets, Carbohydr. Polym. 182 (2018) 1–7.
[35] H. Matsumura, J. Sugiyama, W.G. Glasser, Cellulosic nanocomposites. I., Thermally deformable cellulose hexanoates from heterogeneous reaction, J. Appl. Polym. Sci. 78 (2000) 2242–2253.
[36] P.A. Larsson, L.A. Berglund, L. Wågberg, Ductile All-Cellulose Nanocomposite Films Fabricated from Core-Shell Structured Cellulose Nanofibrils, Biomacromolecules 15 (6) (2014) 2218–2223.
[37] J. Leguy, A. Diallo, J.-L. Putaux, Y. Nishiyama, L. Heux, B. Jean, Periodate Oxidation Followed by NaBH4 Reduction Converts Microfibrillated Cellulose into Sterically Stabilized Neutral Cellulose Nanocrystal Suspensions, Langmuir 34 (37) (2018) 11066–11075.
[38] A. Peterson, A.Y. Mehandzhiyski, L. Svenningsson, A. Ziolkowska, R. Kádár, A. Lund, L. Sandblad, L. Evenäs, G. Lo Re, I. Zozoulenko, C. Müller, A Combined Theoretical and Experimental Study of the Polymer Matrix-Mediated Stress Transfer in a Cellulose Nanocomposite, Macromolecules 54 (7) (2021) 3507–3516.
[39] S. Zhou, K. Tashiro, T. Hongo, H. Shirataki, C. Ya-mane, T. Ii, Influence of Water on Structure and Mechanical Properties of Regenerated Cellulose Studied by an Organized Combination of Infrared Spectra, X-ray Diffraction, and Dynamic Viscoelastic Data Measured as Functions of Temperature and Humidity, Macromolecules 34 (2001) 1274–1280.
[40] D. Battegazzore, J. Alongi, A. Frache, L. Wågberg, F. Carosio, Layer by Layer-functionalized rice husk particles: A novel and sustainable solution for particleboard production, Mater. Today Commun. 13 (2017) 92–101.
[41] H.F. Conway, V.E. Sohns, Pilot-Plant Electrolytic Cell for Producing Dialdehyde Starch, Indust. Eng. Chem. 51 (5) (1959) 637–638.
[42] H. Liimatainen, J. Sirviö, H. Pajari, O. Hormi, J. Niinimäki, Regeneration and recycling of aqueous periodate solution in dialdehyde cellulose production, J. Wood Chem. Technol. 33 (4) (2013) 258–266.
[43] S. Koprivica, M. Siller, T. Hosoya, W. Roggenstein, T. Rosenau, A. Potthast, Regeneration of aqueous periodate solutions by ozone treatment: a sustainable approach for dialdehyde cellulose production, ChemSusChem 9 (8) (2016) 825–833.
[44] Z. Tadmor, Molecular orientation in injection molding, J. Appl. Polym. Sci. 18 (6) (1974) 1753–1772.
[45] WALTER Rose, Fluid–fluid interfaces in steady motion, Nature 191 (4785) (1961) 242–243.